Dynamic analysis of a composite material telecommunications tower under wind loads

João Paulo D. de S. Pereira[1], Eliane Maria L. Carvalho[1], Wendell D. Varela[2], Janine D. Vieira[1]

[1] *Escola de Engenharia, Universidade Federal Fluminense (UFF)*
Rua Passo da Pátria, 156, São Domingos, 24210-240, Niterói/RJ, Brazil
jp_dias@id.uff.br, elianemaria@vm.uff.br, janinedv@id.uff.br

[2] *PEC/COPPE, Universidade Federal do Rio de Janeiro (UFRJ)*
Av. Athos da Silveira Ramos, 149, Cidade Universitária, 21941-909, Rio de Janeiro/RJ, Brazil
wendell@fau.ufrj.br

Abstract. This work aims to analyze a glass fiber reinforced polymer (GFRP) telecommunications tower under wind dynamic loads. The natural frequencies of the structure's first lateral bending modes in both planes, obtained from a numerical model using the Finite Element Method, were less than 1 Hz. According to the Brazilian standard NBR 6123, with those values, a dynamic analysis of the structure under wind fluctuation is necessary. A Python language program was developed in order to simulate the fluctuation of the wind and solve the dynamic equilibrium equations. With the time domain analysis of the tower, large displacements at the top of the tower were identified. To solve this problem, a nonlinear pendulum control system adjusted to the natural frequency of the structure for both planes was designed. The coupled equations of motion of the structure and the controller attached to its top were also implemented in the Python program, obtaining the controlled and uncontrolled structure responses. For a set of random simulations of wind conditions, the efficiency of the nonlinear pendulum control system in reducing displacements amplitudes in the two planes of the structure was assessed.

Keywords: Pultruded composite. Telecommunications towers. Structural dynamics. Dynamic wind action. Vibration attenuators.

1 Introduction

The glass fiber reinforced polymer (GFRP) is a composite material whose main characteristics are a high resistance to corrosion, being suitable for coastal regions, a high strength/mass ratio and a low modulus of elasticity when compared to steel [1]. Tall structures, such as telecommunication towers, are normally very flexible, presenting low natural frequencies and being subject to the phenomenon of resonance with wind loads. A GFRP telecommunications tower under the action of the wind can, therefore, have excessive vibrations that could cause large displacements and even the failure of it. The free vibration analysis of the three-dimensional (3D) numerical model of a GFRP telecommunications tower found a 0.89 Hz natural frequency for the first lateral bending modes in both planes. According to NBR 6123 [2], for natural frequencies under 1 Hz, a dynamic analysis of the structure under wind fluctuating action is necessary. This result was obtained using a commercial program based on the Finite Element Method (FEM), and the dynamic analysis of the structure was then conducted on a simplified two-dimensional (2D) model by a program developed in Python to solve its equation of equilibrium in the time domain.

2 Description of the models

A 3D model of the composite tower was developed in a commercial program based on the FEM in order to obtain the dynamic properties from the free vibration (or modal) analysis. Subsequently, the 3D model was adapted

to a simplified 2D unifilar representation, so that it could be applied in the Python program developed to solve the dynamic equations of equilibrium of the structure under wind fluctuating loads.

2.1 Three-dimensional (3D) model

The 60m high freestanding structure was divided in 20 modules whose cross sections are identified by colors in Fig. 1a and 1b. Figure 1b also shows the 3D model's dimensions. The square base of the tower is 9m wide, with sloping leg members up to 50m height. For the last 10m a constant 2m square section was used. Accessories like coaxial cables, waveguides and GFRP sailor ladder were linearly considered along the structure's vertical axis, and 6 GFRP grid platforms were placed according to a tower design guide by Telebras [3], in relation to the tower's height. Figure 1b also shows the position of the platforms, going from height z_1 to z_6. Following the same design guide, all the antennae were placed 1m above the platforms, and four workers and maintenance equipment were evenly distributed in the two top ones. In total, 12 sector antennae were placed in pairs in a helicoidal pattern (Fig. 1c), and 4 parabolic antennae were placed above the two top platforms.

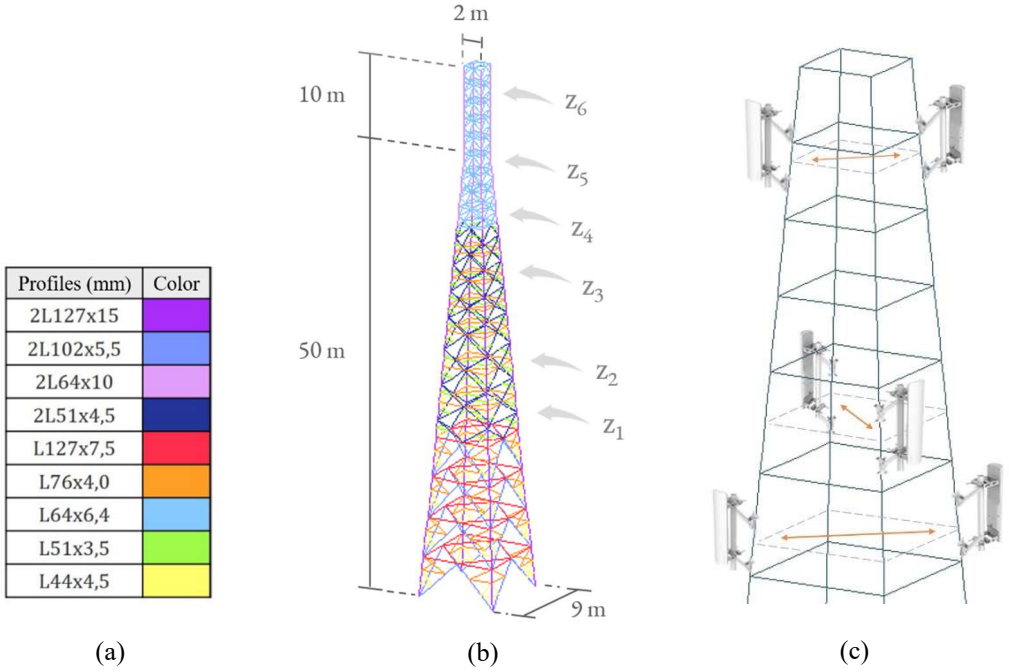

Figure 1. (a) Color legend of the profiles; (b) 3D model's dimensions, cross section distribution and position of the platforms; (c) sector antennae distribution pattern.

The supports were considered clamped, and the connection of the profiles was adopted as rigid between the segments of the leg members and main horizontal bars, and flexible at the ends of the other bars. The profiles, whose dimensions are shown in Tab. 1, ranged between 9 single and double angle sections made of glass fiber reinforced polymer (GFRP). The longitudinal and transversal moduli of elasticity (respectively, E_L and E_t) were obtained based on Cardoso and Togashi experimental data [4], as shown in Tab. 1. For all profiles the shear modulus G = 2.47 GPa and the mass density ρ = 1.8 t/m³ were adopted. The total mass of the tower and its accessories are, respectively, 5.54 t and 7.02 t.

Table 1. Used profiles and their moduli of elasticity.

Profile	E_L (GPa)	E_t (GPa)
2L127x15	27.8	8.62
2L102x8,0	27.8	8.62
2L64x10	27.8	8.62
2L51x4,5	24.6	6.88
L127x9,5	27.8	8.62

L76x4,0	24.6	6.88
L64x6,4	27.8	8.62
L51x3,5	24.6	6.88
L44x4,5	24.6	6.88

2.2 Two-dimensional (2D) model

The simplified 2D unifilar model consists of 20 nodes representing the modules of the tower and placed in their mid-heights (Fig. 2a), with translational degrees of freedom in *x* and *y* directions. From the free vibration analysis of the 3D model, the modal mass $m_1 = 2.61$ t and the eigenvector (or modal shape) φ_1 were obtained for the first bending mode (Fig. 2b) in both planes, due to the structure's symmetrical configuration. The damping ratio $\xi = 1.5\%$ was adopted according to the European prospect for fiber reinforced polymer (FRP) structural profiles EUR 27666 (2016) [5], in absence of experimental data.

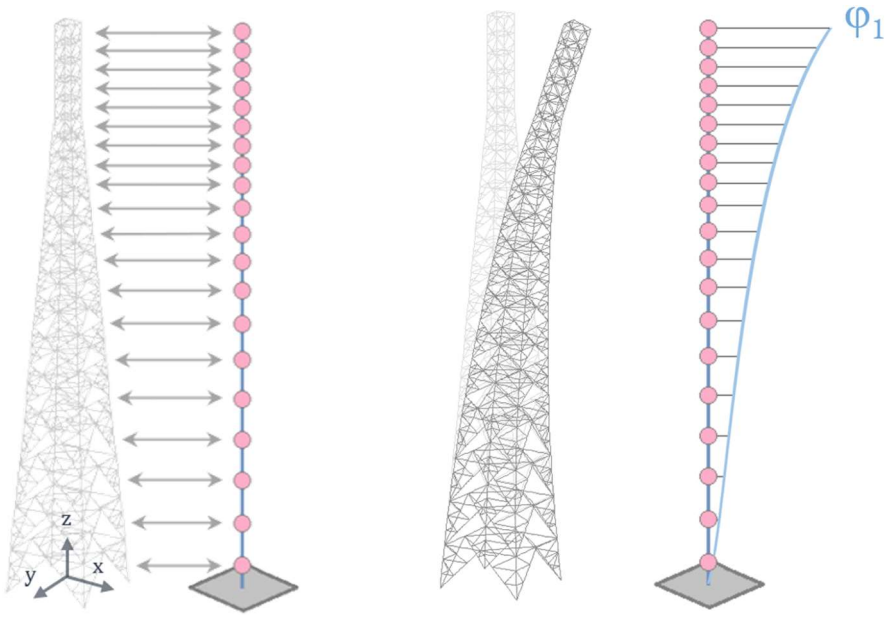

Figure 2. (a) Nodes of the 2D model corresponding to the tower's modules; (b) modal shape of the first bending mode of the tower.

The drag coefficient C_a and the effective wind obstruction area A_e of each module and the associated linear accessories were assigned directly to their corresponding nodes. As for the platforms and antennae, which were not always aligned to the mid-height of the modules, those properties were linearly distributed to the nodes immediately close as shown in Fig. 3.

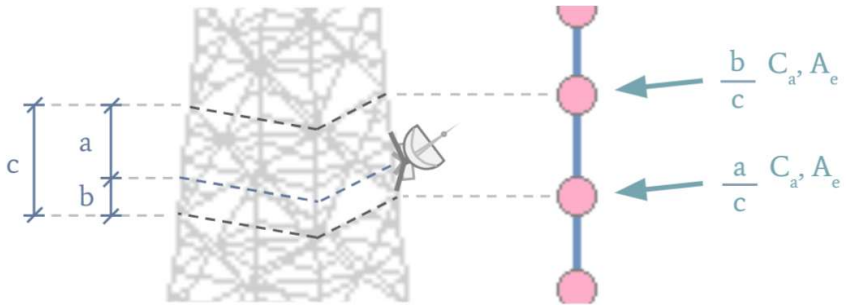

Figure 3. Distribution of the physical properties of the elements not aligned with the node's height.

3 Analysis methodology

The wind drag force F(z,t) was calculated by the following equation:

$$F(z,t) = \frac{\rho\, C_a(z)\, A_e(z)\, [\bar{U}^2(z) + 2\,\bar{U}(z)\, u(z,t)]}{2}. \tag{1}$$

In Eq. (1), ρ is the density of the air, adopted as 1.225 kg/m³. The effective obstruction area A_e and the drag coefficient C_a were defined, respectively, based on the dimension of the components from manufacturers' catalogs and on technical guidelines from Telebras. The average wind speed $\bar{U}$ was calculated according to NBR 6123 for the city of Rio de Janeiro, and the wind fluctuation u(t) was numerically simulated using the Weighted Amplitude Waves Superposition Method (WAWS). In this method, a reduced power spectrum of wind horizontal speed, represented by $S_r(f)$, with the frequency axis in logarithmic scale is subdivided in k = 1, 2, …, N intervals, and the stochastic zero mean signal u(t) is represented by a sum of evenly spaced cosine waves [6]:

$$u(t) = \sum_{k=1}^{N} u_* \sqrt{2\; S_r(f_k)\, \Delta}\; \cdot \cos\,(2\pi\, f_k + \theta_k), \tag{2}$$

where u_* is the friction velocity of the wind, related to terrain roughness, θ_k is a random phase angle with uniform distribution from 0 to 2π, and the cosine waves with central frequencies f_k are weighted by the numerical integral of the spectrum in their associated interval of length Δ. The power spectrum of the wind used in this work, proposed by Davenport after investigation of several horizontal wind speed data [7], is shown below:

$$S_r(f) = \frac{f \cdot\, S(f)}{u_*} = \frac{4\,(1200 + f/U_0)^2}{[1 + (1200 + f/U_0)^2]^{3/4}}, \tag{3}$$

where f is the frequency and U_0 is the average wind speed at a 10m height, measured in m/s. In this work, the spectrum was subdivided in N = 500 intervals. Figure 4 illustrates the numerical integration of Davenport's spectrum for the 6th interval in a N = 10 subdivision, with start and end points at, respectively, 0.035 Hz and 1 Hz.

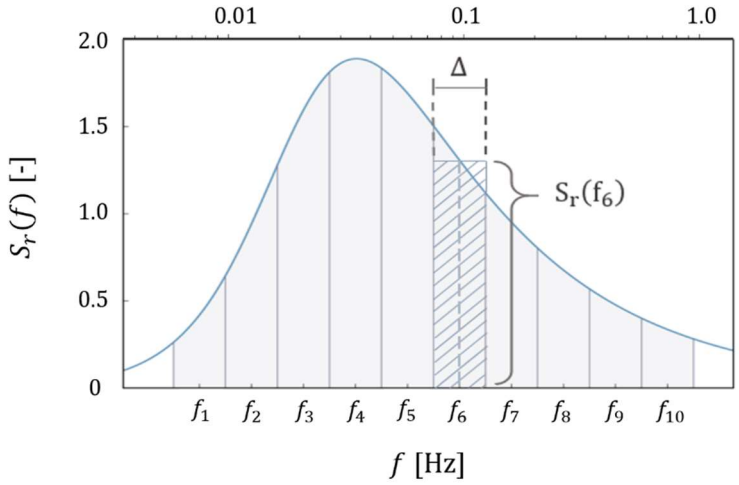

Figure 4. Numerical integration of Davenport's reduced spectrum $S_r(f)$ in N = 10 intervals.

The Modal Superposition Method was used to dynamically analyze the structure. From the condition of orthogonality of a structure's vibration modes, each mode can be analyzed individually for the later superposition of their effects. Considering that only the first bending mode in each plane found a natural frequency lower than 1Hz, being the only modes excited by the wind's fluctuation, the following equation of equilibrium was implemented in the Python program to be solved numerically using the 4th order Runge-Kutta algorithm:

$$\ddot{a}(t) + \alpha\, \dot{a}(t) + \omega^2\, a(t) = \sum_{i=1}^{20} \frac{\rho\, C_{a,i}\, A_{e,i}\, \varphi_i\, [\bar{U}_i^2 + 2\,\bar{U}_i\, u_i(t)]}{2\, m_1}. \tag{4}$$

In Eq. (4), the unknown variable a(t) is independent of height and is called the modal coordinate. The constant α is a proportionality coefficient between mass and damping, having a structural and an aerodynamic part, ω is the angular natural frequency of the analyzed vibration mode and the right side of Eq. (4) is the modal force. After solving the differential equation and finding the structure's modal response in a 10 min interval, the displacement (or physical coordinate) in a certain node *i* can be found through the product of a(t) and the eigenvector's value in that node, φ_i.

To mitigate the structure's response in case of large displacements, a passive attenuator in the form of a non-linear pendulum was designed and placed at the top of the tower. According to Hartog [8], the optimum ratio λ between the attenuator's frequency, f_a, and the structure's natural frequency, f_n, is found through the following equation:

$$\lambda = \frac{f_a}{f_n} = \frac{1}{1+\mu}, \tag{5}$$

where μ is the ratio between the pendular attenuator's mass, m_P, and the structure's modal mass in the analyzed vibration mode. The optimum damping ξ for an attenuator whose frequency is given by Eq. (5) is calculated by the following equation:

$$\xi = \sqrt{\frac{3\mu}{8\,(1+\mu)^3}}. \tag{5}$$

The motion of the structure-pendulum system is described by a pair of coupled equations of equilibrium:

$$\left(m_1 + m_p\right)\ddot{a} + \left(\ddot{\theta}\cos\theta - \dot{\theta}^2\mathrm{sen}\theta\right) m_p\, L + \alpha\, m_1\, \dot{a} + \omega^2\, m_1\, a = f, \tag{6}$$

$$m_p\, L^2\ddot{\theta} + m_p\, L\, \ddot{a}\cos\theta + m_p\, g\, L\, \mathrm{sen}\theta + c_p\dot{\theta} + k_p\theta = 0, \tag{7}$$

where θ(t) is the pendulum's rotational displacement, L is the length of its rod, f is the modal force shown in Eq. (4), g is the gravitational acceleration, c_P is the pendulum's damping constant and k_P its rotational stiffness. Equations (6) and (7) were implemented in the Python program to obtain the response of the structure under control of the non-linear pendulum attenuator.

4 Results and discussion

Due to the high flexibility of the GFRP, the preliminary results for the tower's top displacements pointed the need for a control system. In order to determine the mass of the attenuator, a range of mass ratios μ from 1% to 20% had their efficiency evaluated in mitigating the dynamic displacements of the structure, as shown in Fig. 5. It was found an increase of efficiency with the increase of mass, walking towards an asymptote after μ = 10%. Considering Hartog's suggestion of μ ≈ 10% for a practical attenuator size, the final mass of the attenuator was determined. Table 2 shows the final properties of the non-linear pendulum attenuator and its average values of efficiency and maximum lateral displacement after 2000 runs.

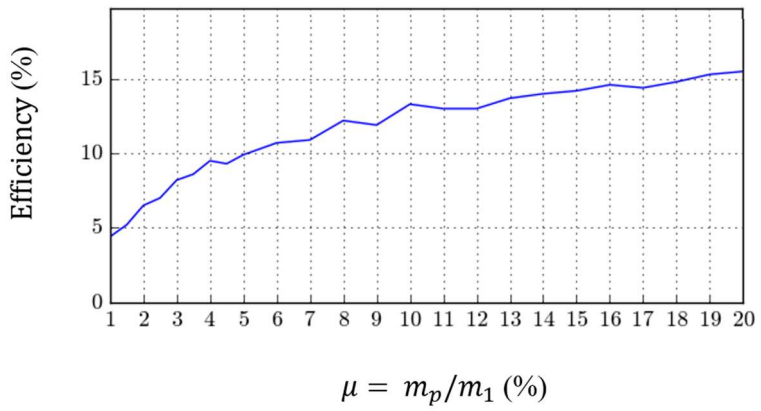

Figure 5. Evaluation of the efficiency of a range of mass ratios μ.

Table 2. Final properties and average results of the non-linear pendulum attenuator.

μ (%)	m_p (kg)	ξ (%)	L (cm)	Efficiency (%)	Max. lateral disp. (cm)
10.0	261	16.8	38.2	13.5 ± 7.6	10.1 ± 0.9

The response at the top of the tower to the time-varying wind load was obtained by the Python program for both the uncontrolled and the controlled structure in the time domain. Figure 6 presents their displacement responses in the frequency domain after going through the FFT algorithm. It can be seen that the presence of the passive control system had no effect in reducing the displacements caused by the low frequency harmonics, even though around the structure's natural frequency (0.89 Hz) the mitigation was considerably good, reaching a reduction of approximately 75% when compared to the uncontrolled structure's resonant amplitude. The acceleration response in the frequency domain, shown in Fig. 7, can help explain why the attenuator's effectiveness was restricted to the region around the resonant harmonics.

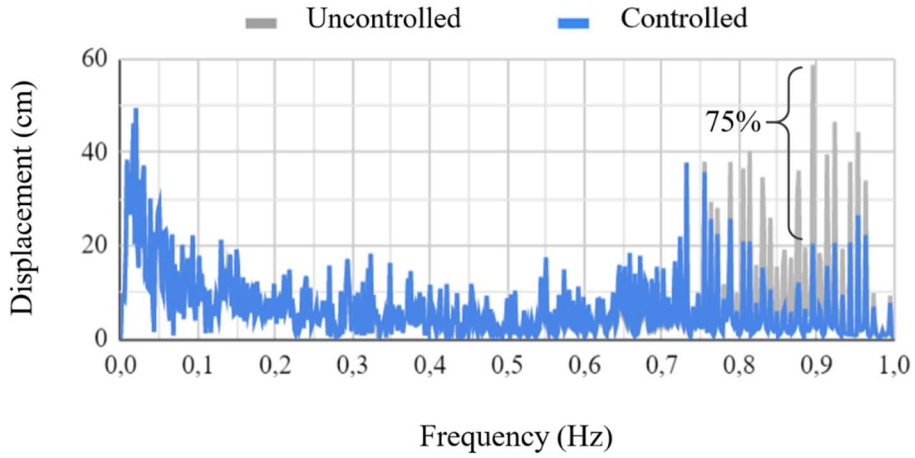

Figure 6. Displacement response at the top of the tower in the frequency domain.

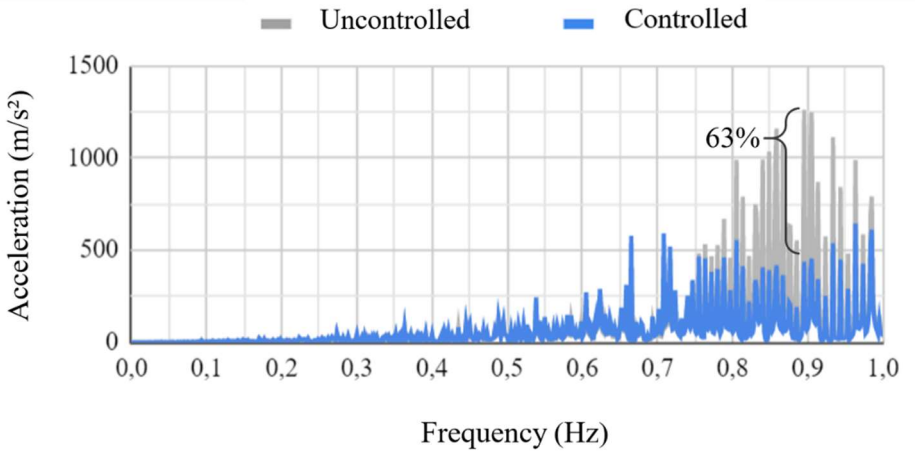

Figure 7. Acceleration response at the top of the tower in the frequency domain.

The low frequency harmonics, especially those lower than 0.2 Hz, were responsible for the largest displacements at the top of the controlled structure (Fig. 6), but Fig. 7 shows they caused no acceleration response. This means that, although the wind load due to those harmonics was time-varying, thus dynamic, the resulting displacements were purely static, and for that reason the passive attenuator adjusted to the structure's natural frequency couldn't act on reducing them.

5 Conclusion

Even not inducing a dynamic response, i.e., without exciting the structure's vibration, the static response brought forth by the low frequency harmonics (distant from the structure's natural frequency) can lead to increasing member stresses and possibly to failure. This deserves attention specially when designing structures in flexible materials as the GFRP. On the other hand, an important aspect to be considered is that the dissipation of kinetic energy promoted by the passive attenuator (Fig. 7) increases the structure's lifespan in relation to fatigue ultimate limit state. The non-linear pendulum, adjusted to the tower's natural frequency, had success in mitigating the dynamic response caused by the resonant harmonics of the fluctuating portion of the wind, reaching a 75% and 63% reduction in the displacement and acceleration responses, respectively, when compared to the uncontrolled structure (Fig. 6 and 7). That shows the importance of designing a passive control system to ensure the safety, comfort and long lifespan of a slender and flexible structure like a GFRP telecommunications tower. It is expected that this kind of control system, when associated to structures with lower natural frequencies, approaching the portion of the spectrum with higher energy concentration - namely, the frequencies around 0.35 Hz (Fig. 4) - tend to reach higher efficiencies, once those harmonics will cause resonant responses upon which the non-linear pendulum attenuator works best.

Authorship statement. The authors hereby confirm that they are the sole liable persons responsible for the authorship of this work, and that all material that has been herein included as part of the present paper is either the property (and authorship) of the authors, or has the permission of the owners to be included here.

6 References

[1] J. M. Jones. "Mechanics of composite materials". McGraw Hill, 2nd ed., pp. 2, 27-31. USA, 1999.
[2] Associação Brasileira de Normas Técnicas. "NBR 6123: Forças devidas ao vento em edificações". 3rd rev. ed., p. 33. Rio de Janeiro, 2013.
[3] Telebras. "Prática 240-410-600: procedimentos de projeto para torres metálicas auto-suportadas, estaiadas e postes metálicos". Sistema de Documentação Telebras, 2nd ed., p. 20. Brasil, 1997.
[4] D. C. T. Cardoso and B. S. Togashi. "Experimental investigation on the flexural-torsional buckling behavior of pultruded GFRP angle columns". Thin-Walled Structures, v. 125, p. 273. Rio de Janeiro, 2018.
[5] L. Ascione, J.-F. Caron, P. Godonou, K. van IJselmuijden, J. Knippers, T. Mottram, M. Oppe, M. Gantriis Sorensen, J. Taby, L. Tromp. "Prospect for new guidance in the design of FRP". EUR 27666 EN. DOI:10.2788/22306.
[6] A. Iannuzzi and P. Spinelli. "Artificial wind generation and structural response". Journal of Structural Engineering, vol. 113, n. 12, pp. 2385-2386, 1987.
[7] A. G. Davenport. "The spectrum of horizontal gustiness near the ground in high winds". Quarterly Journal of the RMetS, vol. 87, n. 372, pp. 195-208. Bristol, 1961.
[8] J. P. D. Hartog. "Mechanical vibrations". McGraw Hill, 3rd ed, pp. 124-131. Cambridge, 1947.